Gd-doped GaN: A very dilute ferromagnetic semiconductor with a Curie temperature above 300 K

S. Dhar,* L. Pérez, O. Brandt, A. Trampert, and K. H. Ploog
Paul-Drude-Institut für Festkörperelektronik, Hausvogteiplatz 5–7, D-10117 Berlin, Germany

J. Keller and B. Beschoten
2. Physikalisches Institut, RWTH Aachen, 52056 Aachen, Germany
(Received 17 August 2005; revised manuscript received 13 October 2005; published 15 December 2005)

We present a systematic study of growth, structural, and magnetic characterization of GaN:Gd layers grown directly on 6H-SiC(0001) substrates by reactive molecular-beam epitaxy with a Gd concentration ranging from 7×10^{15} to 2×10^{19} cm^{-3}. The structural properties of these layers are found to be identical to those of undoped GaN layers. However, the magnetic characterization reveals an unprecedented effect. The average value of the magnetic moment per Gd atom is found to be as high as 4000 μ_B as compared to its atomic moment of 8 μ_B. Such a colossal magnetic moment can be explained in terms of a long range spin polarization of the GaN matrix by the Gd atoms which is reflected by the circular polarization of magnetophotoluminescence measurements. Moreover, the material system is found to exhibit ferromagnetism well above room temperature in the entire concentration range under investigation. We propose a phenomenological model to understand the macroscopic behavior of the system. Our study reveals a close connection between the observed ferromagnetism and the colossal magnetic moment of Gd.

DOI: 10.1103/PhysRevB.72.245203 PACS number(s): 75.50.Pp, 76.30.Kg, 75.50.Dd, 68.55.−a

I. INTRODUCTION

Rare-earth (RE) doping of the wide band gap semiconductor GaN has recently attracted great attention, as light emission extending from the infrared to the blue arising from sharp intra-f-shell optical transitions has been observed.[1,2] Assuming that the RE exists in the RE^{3+} oxidation state in GaN, it was found that the RE readily substitutes Ga leading to electrically inert centers.[3,4] The substitutional RE impurity does not possess any deep gap state. In the current search for ferromagnetic wide band gap semiconductors with a Curie temperature above 300 K, doping with RE elements could be a promising alternative to transition metals (TM). RE atoms have partially filled f-orbitals which carry magnetic moments and may take part in magnetic coupling as in the case of transition metals with partially filled d-orbitals. While it is expected that the magnetic coupling strength of f-orbitals is much weaker than that of d-orbitals due to the stronger localization of f-electrons, Gd is the only RE element which has both partially filled 4f and 5d orbitals. Both the 5d and 4f orbitals can take part in a new coupling mechanism proceeding via intra-ion 4f-5d exchange interaction followed by inter-ion 5d-5d coupling mediated by charge carriers.[5,6] Teraguchi[7] *et al.* have recently observed ferromagnetism in ternary alloy $Ga_{0.94}Gd_{0.06}N$ films with a Curie temperature of 400 K. Moreover, even at this high concentration, Gd was shown to occupy predominantly Ga sites in the hexagonal GaN lattice.

In this paper we present the results of our systematic study of growth and magnetic properties of Gd-doped wurtzite GaN layers with a concentration of Gd ranging from 7×10^{15} to 2×10^{19} cm^{-3}. In the entire concentration range studied here the Gd-doped GaN layers are found to be ferromagnetic with Curie temperatures far above room temperature. Moreover, our magnetization measurements reveal an extremely high magnetic moment of up to 4×10^{3} μ_B per Gd atom.[8] This colossal magnetic moment can be understood in terms of a long-range spin polarization of the GaN matrix by Gd. This interpretation is supported by the pronounced change of the circular polarization in magnetophotoluminescence measurements upon light Gd-doping. A phenomenological model is developed to explain the macroscopic magnetic behavior of the system, demonstrating a close connection between the observed ferromagnetism and the colossal magnetic moment of Gd.

II. EXPERIMENTAL

A. Sample growth and structural characterization

The hexagonal GaN layers of thickness 400–700 nm, and with a Gd concentration ranging from 7×10^{15} to 2×10^{19} cm^{-3} were grown by reactive molecular beam epitaxy (MBE) directly (i.e., without any buffer layer) on 6H-SiC(0001) substrates. The MBE system is equipped with conventional effusion cells for Ga (7N purity) and Gd (4N purity) and an unheated gas injector for NH_3 (9N purity). The base pressure of the chamber reaches 2×10^{-10} Torr with cryoshrouds only around the effusion cells.

The Gd ingot was produced by Stanford Materials Corporation and has a purity of 4N (99.99%) as certified by a chemical analysis (inductively-coupled plasma mass spectroscopy) performed by the manufacturer. The data sheet of our ingot certifies that the ferromagnetic elements Fe and Ni are present in residual traces of $\leqslant 100$ ppm, $\leqslant 50$ ppm, respectively, while the concentrations of the other TMs such as Cr and Co are found to be below the detection limit (0.5 ppm). As we remained below the melting point of Gd

 ©2005 The American Physical Society

(1312 °C) during growth, the evaporation occurs by sublimation and the given values correspond to the ratio of the trace elements to Gd in the GaN layer. In addition, the vapor pressure of Gd, Fe, Ni, Cr, and Co is quite close in the temperature range 1100 to 1500 K. The maximum concentration of ferromagnetic contaminants might thus be in the range of 1×10^{12} to 3×10^{15} cm^{-3} in these samples.

The substrate temperature was kept at 810 °C, which is our standard growth temperature for GaN in this system. The growth rate was set to our standard value of 0.6 μm/hr. The NH_3 flux was regulated to keep the chamber pressure at $4–5\times10^{-6}$ Torr and the Ga cell temperature was kept at 1000 °C during growth. To control the Gd incorporation into the GaN layers, the Gd/Ga flux ratio was adjusted by varying the Gd cell temperature in the range of 950 to 1300 °C. Nucleation and growth of GaN on SiC was monitored *in situ* by reflection high-energy electron diffraction (RHEED). A spotty (1×1) RHEED pattern, reflecting a purely three-dimensional growth mode, was observed during nucleation of the layers. The pattern quickly became streaky, reflecting two-dimensional growth. At this stage, a (2×2) surface reconstruction appears. It is worth noting that all these features in RHEED are also observed when pure GaN layers are grown.[9] An undoped GaN sample for reference purposes was also grown under similar conditions in the sequence of the GaN:Gd samples.

The Gd concentration of the layers was determined by secondary ion mass spectrometry using a CAMECA IMS 4*f* system, employing 0_2^+ primary ions with an impact energy of 7 keV. Mass interference due to parasitic molecular ions was avoided by selecting precisely the masses of two Gd isotopes (155.922 and 157.924). The resulting ion rates were identical to within 1%. Measurements at different locations of the GaN:Gd samples, each of which involved an area of 50×50 μm^2, deviated by no more than 5%. The concentration was calculated according to measurements of an ion-implanted GaN standard (sample I), which was implanted with a Gd dose of 10^{15} cm^{-2}. The detection limit of secondary-ion-mass spectroscopy (SIMS) was found to be 2×10^{15} cm^{-3} for Gd. In order to get an estimate of the concentration of the residual magnetic impurities, one GaN:Gd layer with a high Gd concentration of 1×10^{19} cm^{-3} was scanned in the entire TM and RE series of the periodic table by SIMS. A very low concentration of Cr in the range of 10^{13} cm^{-3} was found in this layer. None of the other TM or RE elements was detected. It has to be noted that the detection limit for Cr in SIMS is low (10^{12} cm^{-3}). For the rest of the TM and RE elements the detection limit is around 10^{15} cm^{-3}. This finding is in accordance with our upper-bound estimate of these impurities from the purity chart of the Gd ingot provided by the manufacturer as stated above.

The structural properties of the layers were investigated by x-ray diffraction (XRD) and transmission electron microscopy (TEM). For TEM, a JEOL3010 microscope operating at 300 kV was used. Symmetric high-resolution triple-axis x-ray $\omega-2\theta$ scans were taken with a Phillips Xpert diffractometer equipped with a Cu $K\alpha_1$ source, a Bartels-type Ge(002) monochromator and a Si(111) analyzer. The dynamic range of these measurements is larger than six orders of magnitude. The surface morphology of the films was examined by atomic force microscopy (AFM) and scanning electron microscopy (SEM).

B. Assessment of electrical and magnetic properties

Magnetization measurements up to 360 K were done in a Quantum Design superconducting quantum interference device (SQUID) magnetometer. The sample holder (a 20 cm long plastic straw provided by Quantum Design) was found to yield no magnetic signal at all. This finding is in accordance with the statement of Quantum Design that the MPMS magnetometer pickup coil (which takes the form of a second-order gradiometer) detects changes of the magnetization induced by a sample, but not the spatially homogeneous diamagnetic signal of the straw itself. The response of the magnetometer was calibrated with thin epitaxial Fe and MnAs layers on GaAs(001) whose magnetization is accurately known. The typical surface area of the samples for the magnetization measurements is 35–40 mm^2. The magnetization of undoped GaN layers was found to be indistinguishable from the diamagnetic response of bare SiC substrates. Magnetization loops were recorded at various temperatures for magnetic fields between ±50 kOe. The magnetic properties of several samples were investigated up to 800 K using a separate Quantum Design SQUID magnetometer equipped with an oven that is specially designed for the high temperature measurements. The magnetic field was applied parallel to the sample surface, i.e., perpendicular to the *c*-axis, in all measurements. All data presented here were corrected for the diamagnetic background of the substrate according to the following procedure: We measured the magnetization of the respective sample up to the highest magnetic field available (±50 kOe). At this high field, the diamagnetic contribution from SiC is dominating the signal. A linear fit yields the slope of the signal at high fields, which in all cases was virtually identical to that of bare SiC substrates. A straight line with the slope determined from the fit was then subtracted from the raw data. Prior to measuring the temperature dependence of the magnetization, the sample was first cooled from room temperature to 2 K either under a saturation field of 20 kOe (Field cooled: FC) or at zero field (zero field cooled: ZFC). In case of ZFC measurements the sample is demagnetized under an oscillatory magnetic field at room temperature before cooling it down to 2 K. Conductivity measurements revealed all samples (including the reference sample) to be electrically highly resistive ($\rho\approx1$ MΩ cm) even at room temperature. Note that the level of oxygen, which acts as unintentional donors in GaN, was found by SIMS to be 1×10^{18} cm^{-3} in these samples including the reference sample.

III. RESULTS AND DISCUSSION

A. Gd incorporation in GaN

Figure 1 shows the SIMS depth profiles obtained for three Gd doped GaN layers *C*, *E*, and *F*. Clearly, the concentration of Gd remains constant over the entire depth. In Fig. 2, the Gd concentration N_{Gd} as measured by the SIMS is plotted as a function of the Gd/Ga flux ratio ϕ. Samples *C*, *E*, and F

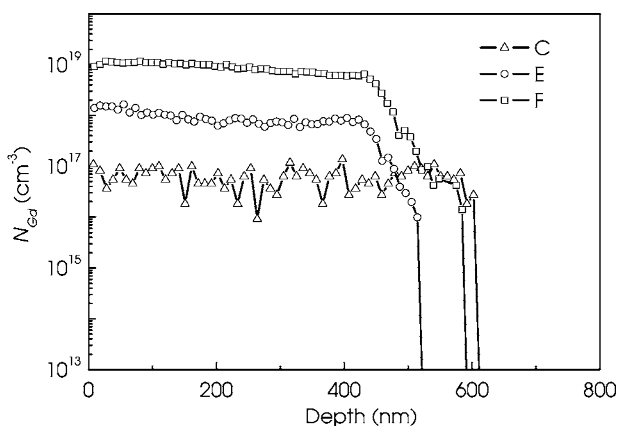

FIG. 1. The SIMS depth profiles for samples C, E, and F.

(solid squares) are lying on a straight line with a slope of unity indicating that the Gd incorporation depends linearly on ϕ up to a Gd concentration of 1×10^{19} cm^{-3}. The Gd concentration of sample G as measured by the SIMS (2×10^{19} cm^{-3}) is found to be smaller than what is expected from this linear dependence. In fact, we have observed a strongly faceted surface for sample G, indicating that Gd is affecting the growth mode at these high concentrations. N_{Gd} for samples A, B, and D (open squares) is obtained by linearly extrapolating the curve passing through samples C, E, and F.

Figure 3 shows the AFM surface image of a GaN:Gd layer with a Gd concentration of 1×10^{19} cm^{-3}. The peak-to-valley and the rms roughness for the 1 μm $\times$ 1 μm scan are found to be 3 and 0.14 nm, respectively. The monolayer steps (about 0.3 nm high) which are clearly visible on the surface, represent an atomically flat surface morphology. It is clear from this figure and the RHEED patterns that the incorporation of Gd in GaN does neither modify the surface reconstruction of the growing GaN layer nor degrade the surface morphology of the 0.5 μm thick film. The surfaces of these films were additionally investigated by the SEM

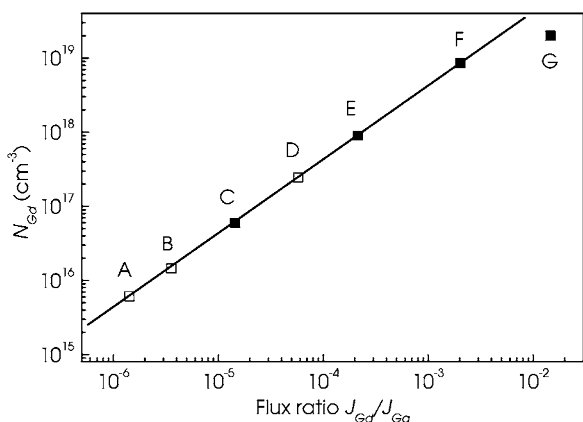

FIG. 2. Gd concentration as measured by the SIMS as a function of Gd/Ga flux ratio (solid squares). The solid line is a linear fit to the data representing samples C, E, and F. The Gd concentration for samples A, B, and D (open squares) is obtained from the corresponding Gd/Ga flux ratio by extrapolation.

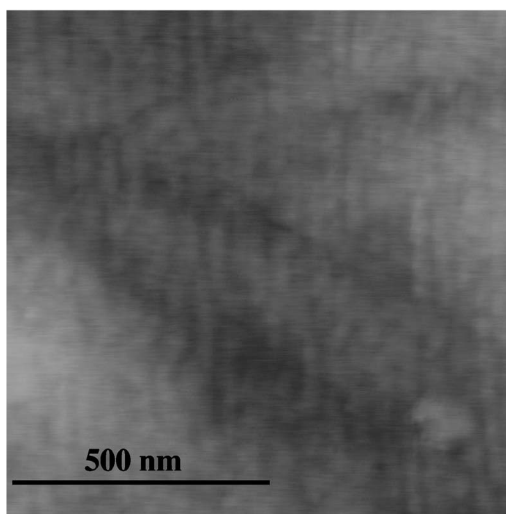

FIG. 3. The AFM surface image of a GaN:Gd film with a Gd concentration of 1×10^{19} cm^{-3}.

(images not shown here) both in topographic and material contrast mode. No contaminating material is found on the surface.

The crystal quality of the samples was investigated by the XRD. Symmetric (0002) and asymmetric $(1\bar{1}05)$ x-ray rocking curves for these samples exhibit a width of 300″ and 900″, respectively, similar to the values observed for equally thin pure GaN layers grown under the same conditions, and comparable to the values reported for high-quality GaN grown by the MBE in general. Figure 4 compares high-resolution triple-axis $\omega-2\theta$ symmetric scans of sample C and the reference sample. Clearly, for both the samples the GaN reflection occurs at the same angular distance from the substrate peak, indicating that the c-lattice constant is not changed by Gd-doping. In fact, it is found that both the in- and out-of-plane lattice constants (measured from asymmetric $[1\bar{1}05]$ scans) remain practically unchanged in all samples from A to F. The incorporation of Gd within that range thus does not influence the crystal quality. However, it is important to note that the c-lattice constant in sample G, which is the highest Gd doped sample in this batch, was

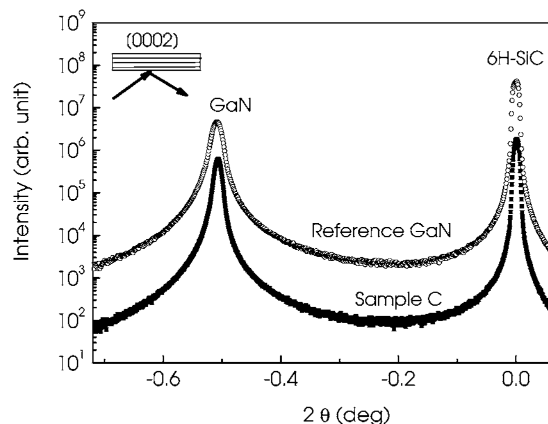

FIG. 4. Symmetric triple-axis $\omega-2\theta$ XRD scans of the reference sample (empty circles) and sample C (solid squares).

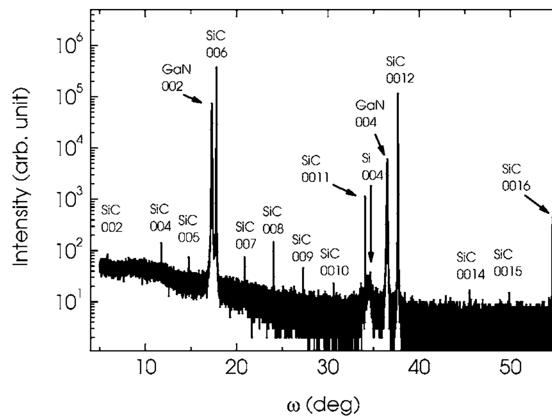

FIG. 5. Symmetric $\omega-2\theta$ XRD scan taken with a 1 mm slit in front of the detector for sample *F*. Note that the Si(004) reflection is originating from the sample holder.

found to be less than that of GaN, while the *a*-lattice constant was found to be practically unchanged.

All samples were subject to an extensive investigation by high-resolution XRD in a wide angular range. Figure 5 shows a symmetric x-ray $\omega-2\theta$ scan taken within a wide angular range of ω from 5° to 55° with a 1 mm slit in front of the detector for sample *F*. Apart from the reflections of the substrate and the layer, no additional reflections related to a secondary phase were detected. Moreover, we have investigated samples *C* and *F* by cross-sectional transmission electron microscopy. Both dark- and bright-field micrographs are taken with different diffraction vectors. No evidence for a secondary phase was found in either of these samples. Figure 6 shows a bright-field TEM micrograph of sample *F* taken with a diffraction vector **g**=[0002]. Clearly, the sample consists of a homogeneous layer without any evidence for a secondary phase. Note that nm-scale Mn-rich clusters were clearly resolved in (Ga,Mn)N layers by the cross-sectional TEM.[10]

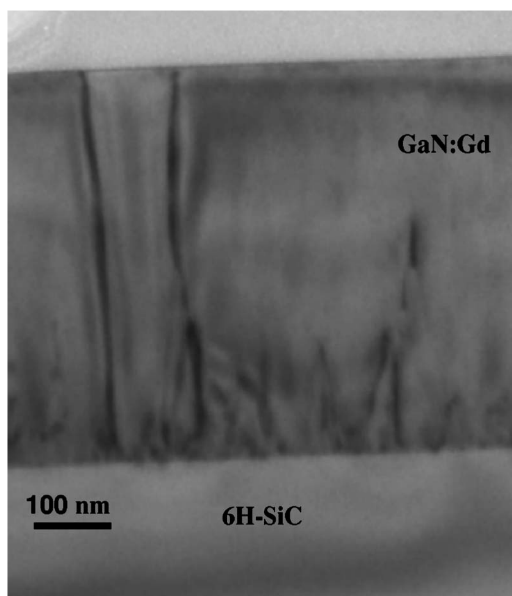

FIG. 6. The bright-field TEM micrograph of sample *F*. The contrast close to the GaN/SiC interface stems from dislocation loops. The dark lines intersecting the micrographs originate from screw dislocations.

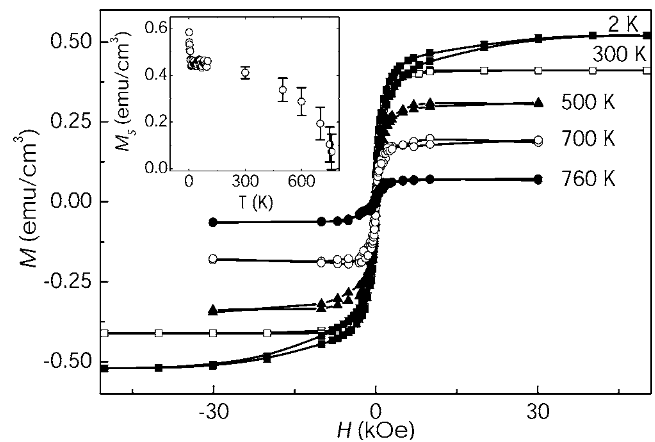

FIG. 7. Magnetization loops obtained for sample *C* at different temperatures. The inset shows the temperature dependence of the saturation magnetization.

B. Magnetic characteristics

Figure 7 shows the magnetization loops obtained for sample *C* at different temperatures. At all temperatures, the magnetization saturates at high magnetic fields and exhibits a hysteresis at lower fields. These two features indicate ferromagnetic behavior. When examined closely it is clear that the shape of the hysteresis loop at 2 K is different from the rest. In Fig. 8 the hysteresis loop obtained at 2 K is compared with the loop at 300 K. The loop obtained at 2 K appears to be a superposition of two loops with different coercive fields (H_c) and remanent magnetizations (M_r). When the temperature is above 10 K, the component with larger H_c and M_r is found to disappear. These findings suggests that there might be two ferromagnetic phases present in the system. The con-

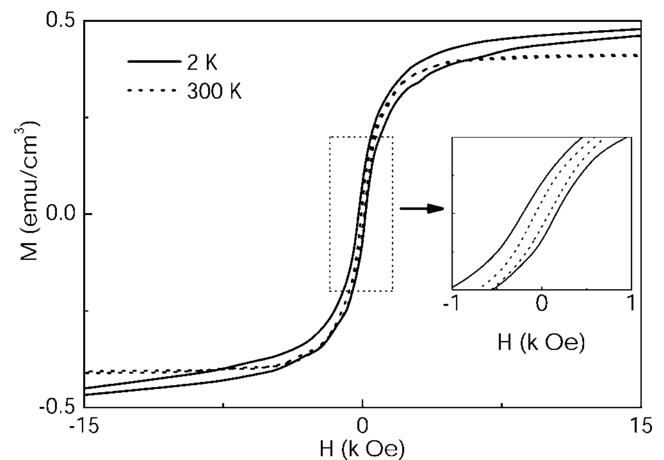

FIG. 8. Comparison of the magnetization loops obtained for sample *C* at 2 K (solid line) and 300 K (dashed line). The inset shows an expanded region of the loops where the hysteresis is clearly visible.

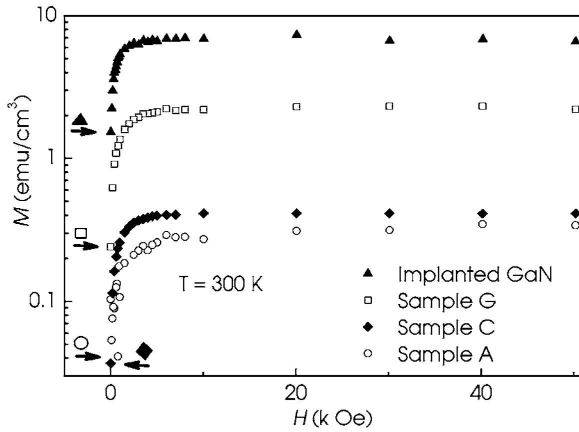

FIG. 9. Part of the full hysteresis loops for samples A, C, G, and I which are obtained when the field decreases from 50 kOe to zero. The positions of M_r are indicated by arrows attached with the respective sample labels.

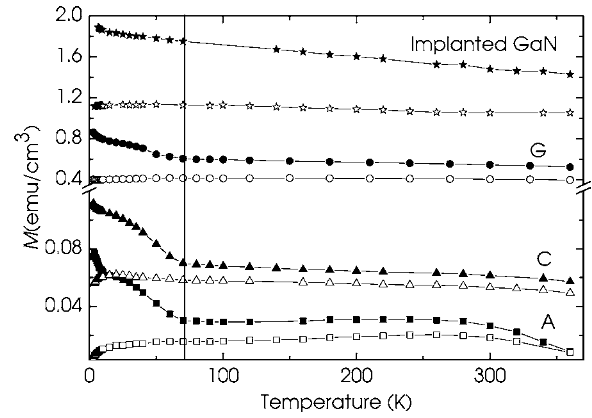

FIG. 10. Temperature dependence of magnetization at field-cooled (solid symbols) and zero-field-cooled (open symbols) conditions at a magnetic field of 100 Oe for samples A, C, G, and I.

tribution with larger H_c and M_r has a T_c around 10 K, while the other contribution can exhibit ferromagnetism even above room temperature. This conclusion is further supported by the upper-left inset of the figure, which shows the saturation magnetization (M_s) as a function of temperature. It is clear from this plot that M_s falls sharply between 2 to 10 K and then decreases slowly as the temperature is increased. A change of slope at 10 K is clearly visible, indicating T_c of the first ferromagnetic component to be around that temperature. Finally, between 700 to 800 K, M_s drops rapidly to zero, marking the Curie point for the second component. All the samples show a qualitatively similar temperature dependence of the hysteresis. It is worth mentioning that the magnetic properties of these samples were investigated in great detail using isothermal remanent magnetization and frequency and field dependent ac susceptibility measurements. Our study reveals that both the phases are indeed ferromagnetic in nature. The results of this detailed study will be reported in a forthcoming paper.[11]

Figure 9 compares the field dependence of the magnetization for samples A, C, G, and I at 300 K. In this figure, only a part of the full loops, which is obtained when the field decreases from +50 kOe to zero, is shown for clarity. Clearly, both M_s and M_r (indicated by arrows) increase as the concentration of Gd increases in these samples. It is worth noting that the Gd-implanted GaN sample (sample I) which is estimated to have a Gd concentration of 1×10^{20} cm^{-3} (more than what we could reach by incorporation during growth) also exhibits ferromagnetism at and well above room temperature.

Figure 10 shows the temperature dependence of the FC and ZFC magnetization under a magnetic field of 100 Oe for samples A, C, G, and I. It is clear from this figure that the FC and ZFC curves are qualitatively similar for all samples featuring a double steplike structure below 70 K in the FC curves. In the case of samples C, G, and I the two curves remain separated throughout the entire temperature range 2 to 360 K, while they coincide at around 360 K for sample A. The separation between the FC and ZFC curves indicates a hysteretic behavior, which is consistent with our observation shown in Fig. 7. The two curves coincide at the Curie temperature T_c, when the hysteresis disappears. Clearly, T_c is around 360 K for sample A while it is much higher for sample C, G, and I. Since the applied field was only 100 Oe for the measurement of the magnetization, the FC curve is expected to qualitatively represent the temperature dependence of M_r. We have also measured M_r directly from the loops obtained at different temperatures which exhibits a similar temperature dependence.[11] The step appearing at 10 K is consistent with our observation of T_c to be around that temperature in case of one ferromagnetic phase as shown in Fig. 7, while the origin of the step at 70 K is not yet clear. It does not seem that a third ferromagnetic phase with T_c around 70 K is additionally present in the system since no step around that temperature is found when M_s is plotted as a function of temperature (Fig. 7).

The separation between the FC and ZFC curves obtained at 360 K is plotted as a function of Gd concentration in Fig. 11. It clearly increases with increasing Gd concentration, revealing a shift of T_c toward higher temperatures. The magnetization as a function of temperature under a magnetic field

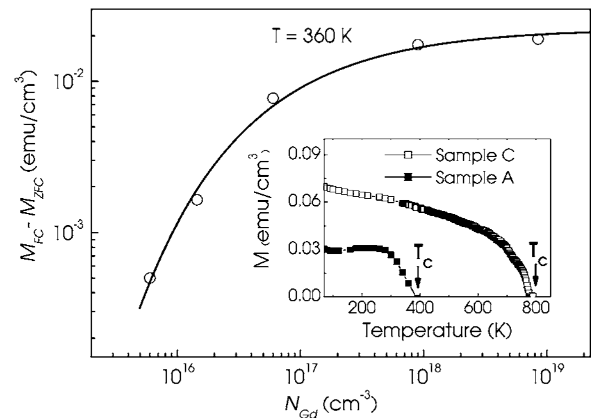

FIG. 11. The difference between FC and ZFC magnetization measured at 360 K plotted as a function of N_{Gd}. The solid curve through the data is a guide to the eye. The inset compares the magnetization as a function of temperature under a magnetic field of 100 Oe for samples A and C.

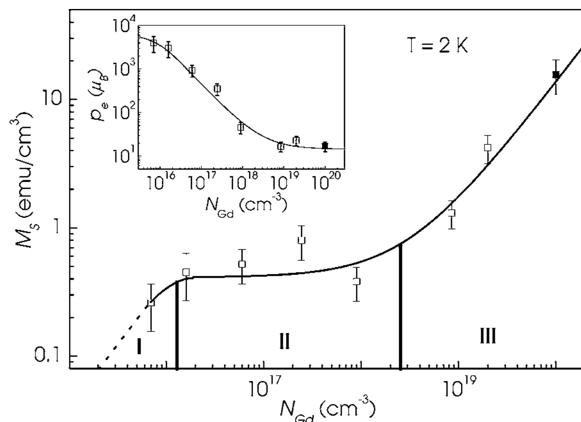

FIG. 12. Saturation magnetization (M_s) as a function of Gd concentration at 2 K. The magnetic moment per Gd atom (p_{eff}) as a function of Gd concentration at 2 K is shown in the inset. Open squares are representing the experimental data for samples *A* to *G* and solid squares for sample *I*. The solid lines are the fits obtained from our model (discussed in the text). Note that the magnetic moment reaches values up to 4000 μ_B for the lowest Gd concentration.

of 100 Oe for samples *A* and *C* is compared in the inset of the figure. The magnetization suddenly drops to zero around T_c indicating a ferro-to-paramagnetic phase transition. This behavior of the temperature dependence of the magnetization is archetypical for a ferromagnet and present in all samples under investigation. T_c is 780 K for sample *C*, which is much larger than T_c (360 K) for sample *A*. This finding is consistent with the data of Fig. 10. In fact, T_c for samples *F* and *G* is found to be also around 780 K.

Figure 12 shows the observed values of M_s at 2 K as a function of Gd concentration. The data obtained from sample *I* are also included in this figure (solid squares). At high Gd concentrations, M_s decreases with the decrease of N_{Gd}. However, below a Gd concentration of about 1×10^{18} cm^{-3}, M_s becomes independent of N_{Gd}. At 300 K a qualitatively similar behavior is observed.[8] The effective magnetic moment per Gd atom p_{eff} obtained from M_s ($p_{\mathrm{eff}}=M_s/N_{\mathrm{Gd}}$) for sample *C* is found to be 935 and 737 μ_B at 2 K and 300 K, respectively. These values are about two orders of magnitude larger than the pure moment of Gd. In the inset of Fig. 12, p_{eff} obtained at 2 K is plotted as a function of N_{Gd}, which is found to be extraordinarily large, particularly for low Gd concentrations, when M_s becomes independent of N_{Gd}. p_{eff} is seen to saturate at high Gd concentrations. It is interesting to note that at 300 K, the saturation value in these heavily Gd-doped GaN samples is close to that of the atomic moment of Gd (8 μ_B), while at 2 K, it is clearly higher. This is true even for sample *I*. Such a colossal moment can be explained in terms of a very effective spin polarization of the GaN matrix by the Gd atoms. Gd atoms are inducing magnetic moments in a large number of Ga and/or N atoms. In fact, in certain diluted metallic alloys, the solute atoms exhibit an average magnetic moment larger than their atomic value. This effect is called giant magnetic moment. There are several reports on a giant magnetic moment of Fe, Mn, and Co when they are either dissolved in or residing on the surface of Pd.[12–14] This effect is explained in terms of a spin polarization of the surrounding Pd atoms. Very recently, a giant moment was observed in Co doped $SnO_{2-\delta}$,[15] a dilute magnetic semiconductor. High-temperature ferromagnetism and an unusually large magnetic moment were observed also in Fe-doped SnO_2, which was argued to originate from a ferrimagnetic coupling mediated by electrons trapped on bridging *F* centers.[16] In the band-structure terminology, the spin polarization of the matrix can be understood as a spin splitting in the conduction and/or valence band. Since our samples are highly resistive, which most likely means that there are no electrons (holes) in the conduction (valence) band, a flat band picture cannot explain the spin polarization even if the band structure is spin-split by Gd. Gd has a larger atomic size than that of Ga, it might be possible that Gd substitution of Ga in GaN produces a large strain field around it. Keeping in mind the large piezoelectric coefficient of GaN along the *c* axis, it is quite plausible that the strain field generates a potential dip around each Gd atom. These potential minima can trap carriers locally. If there is a spin splitting in the band structure, the localized carriers will be spin polarized.

Because of the unexpected nature of our observation, we have in fact proceeded with particular care in all experiments as described in the following.

(i) We have grown more than 40 samples with different Gd concentrations and thicknesses. We also grew many undoped GaN reference samples in between these growth runs. The ferromagnetic signal is found only in Gd doped samples. It is also observed that the magnetization per unit area for a given concentration of Gd scales with the sample thickness.

(ii) We etched the top 120 nm of sample *C* and find similar ferromagnetic behavior for the remaining material. The magnitude of the signal scales nicely with the thickness.

(iii) The surface of these layers was analyzed using three different techniques, RHEED (during growth), AFM, and SEM as mentioned before. Neither Gd nor any other material was found on the surface.

It is clear from the above mentioned observations that the magnetic signal is stemming from the bulk, not from the surface. On the other hand the maximum concentration of ferromagnetic contaminants in these samples is estimated to be on the order of 3×10^{15} cm^{-3} as has been described earlier, which obviously cannot explain the observed magnetization. Note that the magnetization observed in this work for, e.g., samples *A* and *C* would require an Fe (Ni, Co) concentration of 10^{19} cm^{-3} and above, three orders of magnitude higher than the Gd concentration.

The above conclusion of a long-range spin polarization of the GaN matrix by the Gd atoms is independently supported by magneto-photoluminescence (PL) measurements. Magneto-PL measurements were conducted in the Faraday geometry. A magnetic field of 10 T was applied along the *c* direction and the polarization of the photons emitted parallel to the direction of the applied magnetic field was investigated. In the absence of an external magnetic field, the PL spectra of all samples are characteristic for undoped epitaxial GaN layers in that they are dominated by a neutral-donor bound exciton (D^0,X) transition at $\sim$3.458 eV. The lower energy of this transition when compared to homoepitaxial GaN is consistent with the tensile in-plane strain in these

layers of 0.15%.[17] In all cases, the donor responsible for this transition is O with a concentration of about 10^{18} cm^{-3} as measured by the SIMS. However, under the external magnetic field the polarization of the (D^0,X) transition for the Gd doped samples exhibits a different behavior than the undoped GaN sample. As an example, while the (D^0,X) transition is predominantly σ^- polarized for the undoped GaN layer, it is σ^+ polarized for sample C, i.e., the spin splitting of the valence band of the GaN host reverses its sign upon Gd doping. Considering that the mean Gd-Gd separation in sample C is 25 nm, and that the average distance of a (D^0,X) site from a Gd atom will thus be as large as 12 nm,[18] this finding supports our previous conclusion[8] that the Gd atoms are introducing a long range spin polarization in the GaN matrix. These results, together with a quantitative analysis of the dependence of the polarization on the magnetic field, are reported in detail elsewhere.[19]

IV. EMPIRICAL MODEL

In order to get a quantitative understanding of the range of the spin polarization, we have developed a phenomenological model as explained in the following. The polarization of the GaN matrix by the randomly positioned Gd atoms is described as a rigid sphere of influence around each Gd atom, meaning that all the matrix atoms within the sphere are polarized by an equal amount whereas matrix atoms falling outside of this sphere are not affected. Let us associate an induced moment of p_0 with each of the matrix atoms lying in the region occupied by one sphere. As one should expect an increase of the polarization of matrix atoms if they belong to a region where two (or more) spheres of influence overlap, we attribute an additional moment np_1 to matrix atoms occupying sites in regions where n $(n=2,\ldots,N_{\mathrm{Gd}})$ spheres overlap. Since their radius r is presumably much larger than the lattice spacing in GaN, we further assume that the spheres are randomly arranged in a three-dimensional continuum (continuum percolation). Within this framework, the saturation magnetization can be expressed as

$$M_{\mathrm{s}} = p_{\mathrm{Gd}}N_{\mathrm{Gd}} + p_0\tilde{v}N_0 + p_1N_0\sum_{n=2}^{N_{\mathrm{Gd}}} n\tilde{v}_n, \quad (1)$$

where N_0 is the concentration of matrix atoms per unit volume, v is the volume of each sphere, $\tilde{v}=1-\exp(-vN_{\mathrm{Gd}})$ is the volume fraction occupied by the spheres, and

$$\tilde{v}_n = \frac{(vN_{\mathrm{Gd}})^n}{n!}e^{-vN_{\mathrm{Gd}}} \quad (2)$$

is the volume fraction of the regions contained within n spheres. The average magnetic moment per Gd atom p_{eff} is then obtained as

$$p_{\mathrm{eff}} = p_{\mathrm{Gd}} + p_1N_0v + [p_0 - (p_0 + p_1N_{\mathrm{Gd}}v)e^{-vN_{\mathrm{Gd}}}]\frac{N_0}{N_{\mathrm{Gd}}}. \quad (3)$$

On the basis of the behavior of M_s as a function of N_{Gd}, three regimes can be distinguished. At low Gd concentrations (regime *I*), most of the spheres are well separated as shown

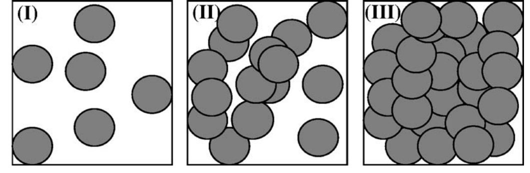

FIG. 13. The panels (I)–(III) represents schematically how the overlap changes as the concentration of Gd increases.

schematically in Fig. 13 (*I*) and p_{eff} has its maximum value. However, in this regime M_s increases with N_{Gd} since $\tilde{v}$ is an increasing function of N_{Gd}. At one point N_{Gd} crosses the percolation threshold and $\tilde{v}$ becomes very close to unity. This point marks the beginning of regime II [Fig. 13 (*II*)]. In this regime M_s remains to be independent of N_{Gd} and p_{eff} decreases as N_{Gd} increases. Finally, at very high Gd concentrations the entire matrix becomes polarized [Fig. 13 (*III*)] and M_s enters into regime III. In this regime, as the first term in Eq. (1) starts to dominate over the rest of the other terms, M_s increases again with N_{Gd} and p_{eff} approaches a saturation. Three regimes are indicated in Fig. 12. Note that in regime III, the value of saturation is larger than the magnetic moment of bare Gd atoms by an amount of p_1N_0v [Eq. (3)]. We use Eq. (1) to fit our experimental data with $p_{\mathrm{Gd}}=8$ μ_{B} and p_0, p_1, and r as free parameters. The agreement is quite satisfactory as shown in Fig. 12. The fit yields $p_0=1.1\times10^{-3}$ μ_{B}, $p_1=1.0\times10^{-6}$ μ_{B}, and $r=33$ nm at 2 K and $p_0=8.4\times10^{-4}$ μ_{B}, $p_1\approx0$, and $r=28$ nm at 300 K.[8] The finite value of p_1 at 2 K explains why p_{eff} saturates at a value which is still higher than the atomic moment of Gd. Most important, however, is that the value of r is sufficiently large to account for the strong effect of Gd on the excitonic ground state of the GaN matrix as has been discussed before.

The second remarkable property of our GaN:Gd layers is the high-temperature ferromagnetism observed in all samples (well above room temperature, compared to a T_{c} of 289 K for bulk Gd). It is clear that the coupling cannot be explained simply in terms of direct, double, or superexchange interaction between Gd atoms since the average Gd-Gd distance is too large for such a coupling to exist. Furthermore, all samples are found to be electrically highly resistive, ruling out free-carrier mediated RKKY(Rudermann-Kittel-Kasuya-Yosida) type long-range coupling. The possibility that the ferromagnetism originates from a Gd-related secondary phase formed by precipitation during growth can also be disregarded for several reasons. First, neither XRD (Fig. 5) nor TEM (Fig. 6) show any evidence for a secondary phase. Second, the Gd concentration in our samples is low, making precipitation extremely unlikely. Third, no (Gd,Ga) or (Gd,N) phases with a T_{c} as high as observed here are known to exist. We believe that the ferromagnetism and the colossal moment of Gd observed in these samples are in fact closely related. An overlap of the spheres of influence establishes a (long-range) coupling between the individual spheres. Within the framework of percolation theory, ferromagnetism is expected to occur at the percolation threshold, when an "infinite cluster" spanning macroscopic regions of the sample is formed. The percolation threshold is reached by our model at $\tilde{v}=0.28955$.[20,21] With increasing Gd concentration, we would

thus expect a phase transition from paramagnetic to ferromagnetic behavior. Furthermore, T_c which depends upon the strength of the overlap is expected to increase with the Gd concentration. This is clearly consistent with the results shown in Fig. 11.

Unfortunately, the well-established percolation formalism cannot be straightforwardly adopted to quantitatively explain the current problem. It is intuitively clear that the spheres of influence are not hard but soft, i.e., the polarization of the matrix induced by the Gd atoms must decay with increasing distance. The onset of ferromagnetic order now depends upon the precise shape of this polarization cloud as well as on the overlap of two or more of these clouds. A quantitative prediction of the onset of ferromagnetism in this situation thus requires a detailed understanding of the nature of the ferromagnetic coupling in this material.

Finally, also very recent proposals aimed at explaining a giant magnetic moment and/or high-temperature ferromagnetism in various material systems[12–16] do not apply to the current requirement of a long-range coupling. An actual understanding of the phenomenon observed in the present paper will require detailed *ab initio* studies, particularly of the *f-d* coupling between Gd and Ga. Considering the long spatial range of the coupling evident from our experiments, such calculations are computationally very demanding and are therefore beyond the scope of the present paper. It could also be possible that the polarization is created not in the matrix atoms but in certain lattice defects generated during growth, such as point defects or complexes. A large density of such defects may form a narrow impurity band in the gap. If the Gd *f* or *d*-orbital is allowed to mix with the band, it could, in principal, generate a spin-splitting there. A large spin polarization could be realized provided that the splitting is more than the width of the band. As has been stated earlier, all our samples, even the undoped GaN layers, are found to be electrically highly resistive, even though a large concentration (more than 10^{18} cm^{-3}) of O (an unintentional donor) is found by SIMS. This finding in fact indicates that a large density of defect states is present in the gap. Here, it is worth mentioning that Venkatesan *et al.*[22] have recently reported an unexpected ferromagnetic behavior in HfO_2, where neither Hf^{4+} nor O^{2+} are magnetic ions, meaning the *d* and *f* shells of Hf^{4+} ions are either empty or full. A similar proposal was introduced in order to explain this unprecedented result.

V. CONCLUSIONS

Our study has revealed an extraordinarily large magnetic moment of Gd in GaN. Since no surface contamination was found and the maximum concentration of magnetic contaminants estimated in these layers is not enough to account for such a large moment, the observed effect cannot be attributed to contamination. Such a colossal moment of Gd arises from a long-range spin polarization of the GaN matrix by the Gd atoms. As a direct result of this effect, the material is ferromagnetic above room temperature even with a Gd concentration less than 10^{16} cm^{-3}. This finding offers an exciting opportunity, since GaN:Gd may be easily doped with donors (acceptors) with a concentration exceeding that of Gd to generate spin polarized electrons (holes) in the conduction band (valence band). Gd-doped GaN with its T_c above room temperature might thus be a very attractive candidate as a source of spin-polarized carriers for future semiconductor-based spintronics.[23]

ACKNOWLEDGEMENTS

We thank M. Ramsteiner, U. Jahn, and K. J. Friedland for important contributions to this work and V. F. Sapega, J. Herfort, M. Bowen, and R. Koch for valuable discussions and suggestions. We also acknowledge partial financial support of this work by the Bundesministerium für Bildung und Forschung of the Federal Republic of Germany. One of us (L.P.) thanks the Alexander von Humboldt Foundation, Germany for financial support.

*Electronic address: dhar@pdi-berlin.de

[1] P. N. Favennec, H. L. Haridon, M. Salvi, D. Moutonnet, and Y. Le Guillou, Electron. Lett. **25**, 718 (1989).
[2] Y. Q. Wang and A. J. Steckl, Appl. Phys. Lett. **82**, 402 (2003).
[3] J. S. Filhol, R. Jones, M. J. Shaw, and P. R. Briddon, Appl. Phys. Lett. **84**, 2841 (2004), and references therein.
[4] M. Hashimoto, S. Emura, R. Asano, H. Tanaka, Y. K. Zhou, N. Teraguchi, A. Suzuki, Y. Nanishi, T. Honma, N. Umesaki, and H. Asahi, Phys. Status Solidi C **7**, 2650 (2003).
[5] T. Story, M. Gorska, A. Lusakowski, M. Arciszewska, W. Dobrowolski, E. Grodzicka, Z. Golacki, and R. R. Galazka, Phys. Rev. Lett. **77**, 3447 (1996).
[6] H. S. Li, Y. P. Li, and J. M. D. Coey, J. Phys.: Condens. Matter **3**, 7277 (1991).
[7] N. Teraguchi, A. Suzuki, Y. Nanishi, Y. K. Zhou, M. Hashimoto, and H. Asahi, Solid State Commun. **122**, 651 (2002).
[8] S. Dhar, O. Brandt, M. Ramsteiner, V. F. Sapega, and K. H. Ploog, Phys. Rev. Lett. **94**, 037205 (2005).
[9] A. Thamm, O. Brandt, Y. Takemura, A. Trampert, M. Ramsteiner, and K. H. Ploog, Appl. Phys. Lett. **75**, 944 (1999).
[10] S. Dhar, O. Brandt, A. Trampert, K. Friedland, K. H. Ploog, J. Keller, B. Beschoten, and G. Güntherodt, Appl. Phys. Lett. **82**, 2077 (2003).
[11] L. Pérez *et al.* (unpublished).
[12] G. Bergmann, Phys. Rev. B **23**, 3805 (1981).
[13] J. Flouquet, O. Taurian, J. Sanchez, M. Chapellier, and J. L. Tholence, Phys. Rev. Lett. **38**, 81 (1977).
[14] J. Crangle and W. R. Scott, J. Appl. Phys. **36** 921 (1965).
[15] S. B. Ogale, R. J. Choudhary, J. P. Buban, S. E. Lofland, S. R. Shinde, S. N. Kale, V. N. Kulkarni, J. Higgins, C. Lanci, J. R. Simpson, N. D. Browning, S. Das Sarma, H. D. Drew, R. L. Greene, and T. Venkatesan, Phys. Rev. Lett. **91**, 077205 (2003).
[16] J. M. D. Coey, A. P. Douvalis, C. B. Fitzgerald, and M. Venkatesan, Appl. Phys. Lett. **84**, 1332 (2004).

[17] P. Waltereit, O. Brandt, A. Trampert, M. Ramsteiner, M. Reiche, M. Qi, and K. H. Ploog, Appl. Phys. Lett. **74**, 3660 (1999).

[18] It can be easily shown that the average distance of an exciton binding site from its nearest Gd ion is $=0.480296a$, where a is the average Gd-Gd separation.

[19] V. Sapega *et al.*, cond-mat/0509198 (unpublished).

[20] R. Consiglio, D. R. Baker, G. Paul, and H. E. Stanley, Physica A **319**, 49 (2003).

[21] D. R. Baker, G. Paul, S. Sreenivasan, and H. E. Stanley, Phys. Rev. E **66**, 046136 (2002).

[22] M. Venkatesan, C. B. Fitzgerald, and J. M. D. Coey, Nature (London) **430**, 630 (2004).

[23] S. A. Wolf, D. D. Awschalom, R. A. Buhrman, J. M. Daughton, S. von Molnár, M. L. Roukes, A. Y. Chtchelkanova, and D. M. Treger, Science **294**, 1488 (2001).